Bioresource Technology 435 (2025) 132893

Contents lists available at ScienceDirect

Bioresource Technology

journal homepage: www.elsevier.com/locate/biortech

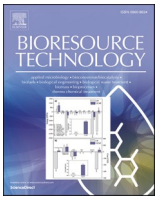

Comparative evaluation of digestate and reject water as nutrient media for syngas biomethanation in thermophilic trickle-bed reactors☆

Florian Gabler [a,b,*], George Cheng [c], Leticia Pizzul [b], Anna Schnürer [c], Åke Nordberg [a]

[a] Department of Energy and Technology, SLU, Box 7032, 750 07 Uppsala, Sweden
[b] Department of Biorefinery and Energy, RISE, Box 7033, 750 07 Uppsala, Sweden
[c] Department of Molecular Science, BioCenter SLU, Box 7015, 750 07 Uppsala, Sweden

HIGHLIGHTS

- High Methane Evolution Rate (4.5 L/(L_{pbv}·d)) achieved using digestate as nutrient.
- High H_2 and CO conversion rates (>95 %) attained using digestate as sole medium.
- Adding S and P to reject water improved MER from 1.0 to 3.1 L/(L_{pbv}·d).
- *Methanothermobacter* was the most abundant methanogen in both reactors.
- Syntrophic acetate oxidation was a key function for efficient gas conversion.

GRAPHICAL ABSTRACT

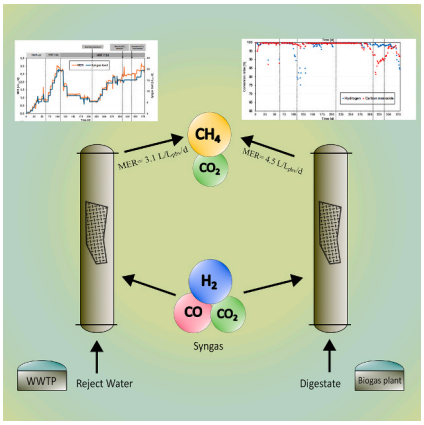

ARTICLE INFO

Keywords:
Biosyngas
Hydrogen
Carbon Monoxide
Sulfur
Microbial Community
Phosphorus

ABSTRACT

Syngas biomethanation facilitates the utilization of thermal gasification products. This study evaluated the performance of two liquid organic waste streams (manure-based digestate and reject water from digested sewage sludge) as nutrient media in thermophilic trickle-bed reactors (TBRs) over more than one year. Digestate achieved a Methane Evolution Rate (MER) of 4.5 L/(L_{pbv}·d) with the highest so far published H_2 and CO conversion rates (>95 %). Reject water only led to a maximum MER of 1.0 L/(L_{pbv}·d), while the addition of sulfur and phosphorus to the reject water resulted in improved MER of up to 3.1 L/(L_{pbv}·d). The microbial analysis illustrated a similar microbial community structure and methanogenic abundance for both TBRs, with *Methanothermobacter* as the dominating methanogen both in the liquid phase and biofilm of the carriers. Carbon monoxide was likely converted to both methane and acetate.

☆ This article is part of a special issue entitled: 'Innovative Biogasprocess' published in Bioresource Technology.

* Corresponding author at: Department of Energy and Technology, SLU, Box 7032, 750 07, Uppsala, Sweden.
E-mail address: florian.gabler@slu.se (F. Gabler).

https://doi.org/10.1016/j.biortech.2025.132893
Received 31 January 2025; Received in revised form 25 June 2025; Accepted 25 June 2025
Available online 25 June 2025

1. Introduction

Syngas originating from the thermochemical conversion of biomass is typically comprised of hydrogen (H_2), carbon monoxide (CO), carbon dioxide (CO_2), and additional gases like nitrogen (N_2) and methane (CH_4). Syngas can be utilized as an energy source, but is also used as an intermediate product for the further processing of high-value products like CH_4 or acetate (Aryal et al., 2021; Andreides et al., 2024). The route for CH_4 production from syngas can turn a variety of low-biodegradable and recalcitrant biomass, like lignocellulosic material or municipal waste, into a versatile energy carrier, increasing synergies with current gas infrastructure for energy storage and distribution (Ren et al., 2020).

Both chemical and biological processes can be used for the methanation of syngas: chemical methanation through catalytic mechanisms or biomethanation mediated by methanogenic archaea (Ren et al., 2020). Compared to chemical-catalytic methods, biomethanation offers the advantage of operating under mild conditions, such as low pressures and temperatures (Grimalt-Alemany et al., 2017). Additionally, biomethanation is more resilient to contaminants like tar and hydrogen sulfide (H_2S) than chemical conversion (Grimalt-Alemany et al., 2017).

During syngas biomethanation, hydrogenotrophic methanogens convert H_2 and CO_2 to CH_4 at a broad temperature range, but the same substrates can be utilized by acetogens for the production of acetate, creating competition for H_2. Methanogens have an advantage over acetogens as they can metabolize lower levels of dissolved hydrogen, due to thermodynamics and substrate affinities (Wegener Kofoed et al., 2021). However, at higher hydrogen levels, acetogens become more competitive for H_2 than methanogens (Liu et al., 2016). The produced acetate can be directly converted into CH_4 by acetoclastic methanogens or via H_2 and CO_2 through a complex biocatalytic reaction chain involving syntrophic acetate-oxidizing (SAO) bacteria and hydrogenotrophic methanogens (Westerholm et al., 2019). Due to thermodynamic restrictions, the SAO conversion route can only function at very low hydrogen partial pressures (Westerholm et al., 2019).

CO can be directly converted to CH_4 by a few hydrogenotrophic methanogens. Between 55 °C and 70 °C, CO is usually converted to CO_2 by carboxydotrophic hydrogenogens (biological water-to-gas shift) (Sipma et al., 2003). The pathway through intermediate products dominates CO conversion due to the favorable thermodynamic conditions of CO-converting bacteria as compared to direct CO transformation by carboxydotrophic hydrogenogens (Sancho Navarro et al., 2016). High CO partial pressure can potentially limit biomethanation because of its toxicity to methanogens and its competition with H_2 as an electron donor.

The slow kinetics of methanogens and the temperature-dependent low liquid–gas mass transfer limit CH_4 productivity. Despite lower gas solubility at higher temperatures, the biological conversion of syngas is faster at 55 °C compared to 37 °C due to higher microbial activity under thermophilic conditions (Sipma et al., 2003). To circumvent mass transfer limitations, the trickle-bed reactor (TBR) is a viable reactor design for biomethanation (Feickert Fenske et al., 2023b). TBRs are gas-tight columns filled with carrier material covered by microbes, over which a nutrient liquid is trickled at different frequencies. The carriers provide a high specific surface (in relation to the reactor volume) for the biofilm to grow on, strengthening the gas–liquid phase boundary interaction (Strübing et al., 2017).

It is essential to supply enough nutrients with the liquid medium to develop microbial activity and growth while either converting syngas or only H_2 and CO_2, which represent carbon and energy sources (Wegener Kofoed et al., 2021). Both macro- and micronutrients that are essential for microbial activity, such as nitrogen (N), sulfur (S), phosphorus (P), and various salts and trace elements, should be present. Several studies have examined biomethanation using a defined nutrient media (Burkhardt et al., 2015; Rachbauer et al., 2016; Asimakopoulos et al., 2019). However, more accessible and economically feasible nutrient sources such as digestate, manure, or reject water from sludge processing at wastewater treatment plants (WWTP) are needed for process upscaling.

The utilization of such non-defined nutrient media, especially digestate or manure, has been assessed satisfactorily for the biomethanation of H_2 and CO_2 (Feickert Fenske et al., 2023b). For the biomethanation of syngas, the use of digestate as a nutrient source has seen interest in recent years (Aryal et al., 2021; Figueras et al., 2021; Andreides et al., 2022a; Cheng et al., 2022; Ali et al., 2024; Goonesekera et al., 2024). Another representative of non-defined media is reject water, which contains high levels of N. For TBR biomethanation systems, reject water as a nutrient medium has only been assessed in three previous studies. The studies by Kamravamanesh et al. (2023) and Feickert Fenske et al. (2023a) used reject water for TBR biomethanation of H_2 and CO_2 and added trace elements stock solutions, whereas the study of Cheng et al. (2022) indicated that the addition of Na_2S to the reject water increases syngas conversion rates and CH_4 productivity. However, there is a need for more comprehensive studies of the digestate and reject water macronutrient supply using the same TBR setup and inoculum for comparison of syngas conversion and CH_4 productivity, to identify potential nutrient limitations.

The objective of the present study was to assess and compare H_2 and CO conversion, and the CH_4 production of syngas biomethanation in continuous long-term (ca. one year) operated thermophilic TBR (V_{pbv} = 5 L) using either digestate or reject water as the nutrient media. Furthermore, indications of performance limitations caused by shortages of S and P in reject water were studied by the supplementation of these macronutrients. Moreover, an additional objective was to study the long-term development of the microbial community with a focus on potential differences depending on the nutrient media.

2. Materials and methods

2.1. Inoculum and syngas

To achieve a broad microbial spectrum covering both mesophilic and thermophilic conditions, a mixture of 4 different digestates was used as inoculum: (A) digestate from the thermophilic digestion of agricultural substrates and municipal food waste (More Biogas Småland AB, Läckeby, Sweden), (B) digestate from thermophilic municipal food waste digestion (Uppsala Vatten och avfall AB, Sweden), (C) digestate from mesophilic manure-based digestion (SLU, Lövsta, Uppsala, Sweden), and (D) digestate from mesophilic sewage sludge digestion (Uppsala Vatten och avfall AB, Sweden). Before mixing, the digestates were filtered through a mesh column (4/2/1 mm) to remove large particles and were subsequently stored for a degassing period of three weeks at 55 °C (digestates A and B) or 37 °C (digestates C and D). The digestates were combined in equal proportions of 25 vol%, and the final mixture was used as inoculum. The characterization of the inoculum is presented in Table S1 (supplementary Material). The utilized syngas was an artificial mixture supplied by Air Liquide (Paris, France) with 40 % H_2, 30 % CO, 20 % CO_2, and 10 % N_2, which can reflect an industrial syngas mixture according to the GoBiGas project, utilizing forestry biomass as gasification substrate (Larsson et al., 2019).

2.2. Nutrient media

The characterization of both nutrient media is presented in Table S1 (SM). The digestate was collected from a mesophilic biogas reactor (SLU, Lövsta, Uppsala, Sweden), mainly operating with manure from pigs and cows. Batches of approximately 60 L were collected at the beginning of the trial, and on day 126 for subsequent storage at 2 °C. Before application to the reactor, the digestate was filtered through a mesh column (4/2/1 mm), diluted with 50 % tap water to reduce the risk of clogging in the reactor, and subsequently stored at 6–8 °C before it was added to the reactor.

Reject water from the sewage sludge dewatering process at a

wastewater treatment plant (WWTP) in Uppsala, Sweden, was collected as two batches of approximately 60 L each at the beginning of the trial and on day 115; these were subsequently long-term stored at 2 °C. The reject water was not filtered or diluted before being added to the reactor. As for digestate, the reject water was moved to a 6–8 °C fridge before addition to the reactor.

2.3. Trickle-bed reactor setup

Two identical acid-proof stainless-steel TBRs were constructed and placed in a movable container together with all associated equipment (Fig. 1). The reactors had a total volume of 7.5 L (an inner diameter of 72 mm and a total height of 1782 mm), including a liquid reservoir of 1 L, which was separated from the packed bed with a grid installed at a height of 504 mm from the bottom. A similar H:D ratio has been used by e.g. Asimakopoulos et al. (2021). For biofilm growth, polyethylene carrier material AnoxKaldnes K1 500 (10 mm diameter, surface area 500 m^2/m^3, density 1.2 g/m^3) was used to create a total packed bed volume (pbv) of 5 L. The nutrient liquid was intermittently recirculated using a progressive cavity pump (Nova Rotors, MN 015–1, 0.6 kW; Sossano, VI, Italy) from the reservoir to the top of the reactor, where it was sprinkled over a perforated metal distribution plate and then trickled downwards through the packed bed to the liquid reservoir. Intermittent liquid trickling was chosen to reduce gas–liquid mass transfer limitations (Sieborg et al., 2021; Goonesekera et al., 2024). The pumps for liquid recirculation were operated with a frequency exchanger in semi-continuous mode with 20 s of pumping every 10 min at an average flow of 40 L/h, recirculating 222 mL per trickling occasion and resulting in a nutrient liquid load of 6.4 $L/(L_{pbv} \cdot d)$. The fresh nutrient medium was pumped into the liquid reservoir 4 to 6 times per day using peristaltic pumps (WMC, 200 Series, Southwick, UK), depending on operational conditions within the corresponding periods. Nutrient supplements were added using adjustable peristaltic pumps (Aalborg TPUA-010005, Orangeburg, US).

The syngas load was controlled by a calibrated mass flow regulator (MFR, Aalborg DPC17; Orangeburg, US) and was continuously added through a port between the liquid reservoir and the packed bed (Fig. 1) to meet the liquid coming from the top, thus operating in a counter-current manner. There was no significant overpressure applied to the TBRs. At the top of the reactor and above the packed bed, the product gas was collected, and after passing a condensed water trap, its volume was measured using a drum meter (TG 0.5; Ritter, Germany) before passing a second condensed trap and entering the gas storage. The composition of the product gas was analyzed for CH_4, CO_2, CO, O_2, and H_2 using an ETG MCA 100 Syn Biogas Multigas Analyzer (ETG Risorse e Tecnologia, Chivasso, Italy) in batches of ca. 3 L from the gas storage. The concentration of H_2S was followed regularly using Kitagawa Gas Detector Tubes No.120SD (Komyo Rikagaku Kogyo, Japan).

The reactors were equipped with three larger ports to allow sampling of carrier material at the top, middle and bottom of the packed bed (Fig. 1). Both TBRs were heated by a water jacket and the temperature in the reactors was logged using three digital temperature sensors at the bottom, middle and top of the TBRs. The nominal temperature monitored in the middle of the TBR was 56 ± 1°C for the entire experiment. A pH electrode (Greisinger GPHU 014 MP-BNC pH electrode, Regenstauf, Germany) was placed in line with the outer recirculation circuit just after the recirculation pump (Fig. 1). Operational control of all pumps was achieved through a microcontroller and software by Arduino (Version 1.8.15; Italy). For the data collection of gas composition, pH, and temperature, the software LabVIEW (National Instruments, Austin,

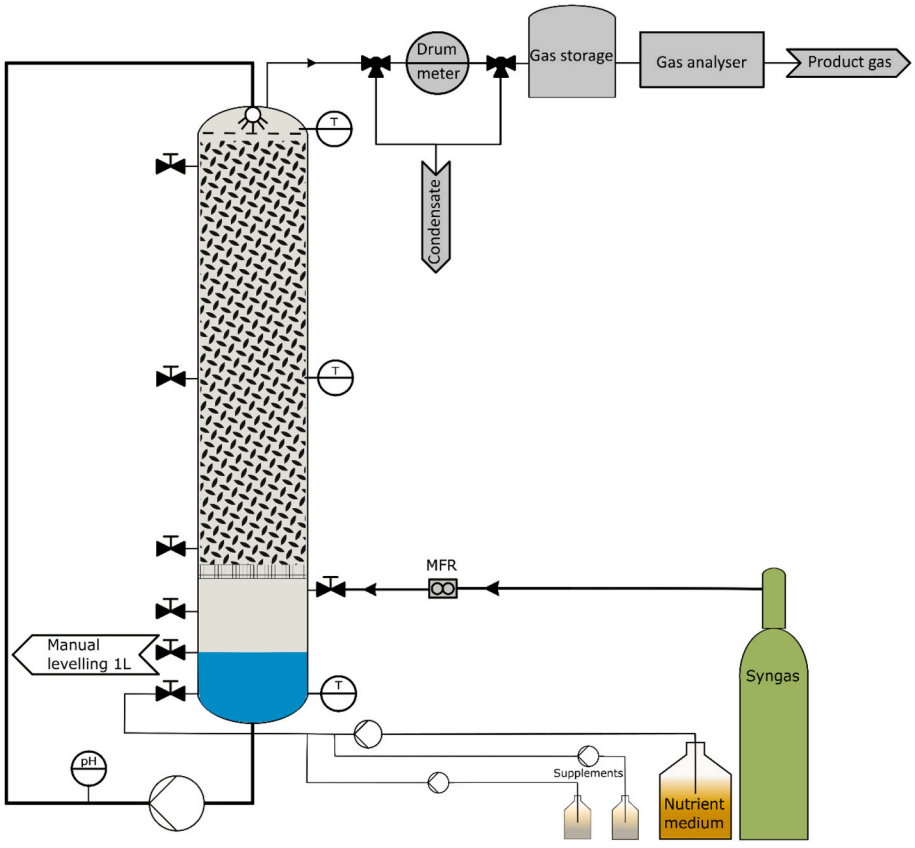

Fig. 1. Process and instrumentation scheme of the trickle-bed reactor (TBR) design. Syngas was supplied to the TBR from a gas cylinder using a mass flow regulator. The liquid medium was intermittently recirculated from the liquid reservoir (V = 1 L) to the top of the trickle bed column. The gas flow was in a counter-current direction to the trickling liquid from bottom to top. The product gas left the reactor at the top, followed by a water trap, volume measurement, and gas dome. Fresh nutrient medium and supplements were pumped intermittently into the liquid reservoir using a peristaltic pump.

US) was used. Volumetric data originating from the MFRs and drum meters was manually documented on working days.

2.4. Process operation

Both reactors were flushed with N_2 (flow rate 20 mL/min) for 24 h before inoculation. The initial 62 days of operation (start-up) were devoted to inoculation of the reactors, which started with the addition of 1.7 L of inoculum to each TBR, followed by a stepwise increase of syngas load (Fig. 2a and 3a). During the start-up period (until day 62), no external nutrient sources were added to the TBRs, and only internal and intermittent (as described in section 2.3) recirculation of the inoculum was performed to establish biofilm growth and adaptation to the environment. Thereafter, the reactors were operated on fresh diluted digestate (TBR1) and reject water (TBR2). Their operation was categorized in several periods based on the hydraulic retention time (HRT) for the nutrient media and the addition of nutritional supplements, as summarised in Table S1, SM. Both TBRs started with an HRT of 15 d, which was based on prior experiences of using non-defined nutrient media for syngas biomethanation. Due to the unstable operation of TBR2 and to assess S and P shortages in the reactor liquid, supplementary sulfur (Na_2S, Merck, Darmstadt/Germany) and phosphorous (KH_2PO_4, Merck, Darmstadt/Germany) were added to TBR2 (Table 1). TBR1 and TBR2 were operated for a total of 370 days and 381 days, respectively.

The major operational guideline applied was to maintain high H_2 and CO conversion rates (above 90 %) throughout the experiment. The adjustment of process parameters such as syngas load or nutrient addition rate was based on the development of H_2 and CO conversion rates, accompanied by changes in the methane evolution rate (MER).

2.5. Sampling and analytical methods

Process liquid was manually removed from the liquid reservoir regularly (every 3–4 days) and was used for chemical and microbial analyses. Analyses of ammonium (NH_4^+) and sulfate (SO_4^{2-}) were conducted straight after sampling from the TBRs, whereas samples used for analyses of phosphate (PO_4^{3-}), volatile fatty acids (VFA) and microbial community were stored at −18 °C. Carriers from the TBRs were sampled on two occasions (day 210 and the end of the trial, i.e. day 371 for TBR1 and day 382 for TBR2) by opening the valves at the top, middle and bottom of the reactor (Fig. 1) while flushing with N_2 (5 mL/min) followed by replacement with fresh carriers.

NH_4^+, SO_4^{2-}, and PO_4^{3-} were analysed using a spectrophotometer (Spectroquant® Nova 60A photometer; MilliporeSigma, Burlington, Massachusetts, United States) with reagent test kits from the series Supelco (Merck, Darmstadt, Germany). Total alkalinity was calculated as the amount of acid required to bring the sample to pH 4.4 based on titration with an automatic titrator (TitraLab® AT1000 series; Hach, Düsseldorf, Germany). Concurrently, pH was measured using a Hanna instrument HI83141 (Woonsocket, Rhode Island, United States). Volatile fatty acids were analyzed through high-performance liquid chromatography according to Westerholm et al. (2012).

Table 1
Chronology of operational changes of TBR1 and TBR2 during the comparison of their syngas biomethanation performance.

Duration [d]	TBR1	TBR2
0	Start inoculation; only internal recirculation	
62	Addition of diluted digestate(HRT 15 d)	Addition of reject water (HRT 15 d)
109		Increase nutrient addition rate (HRT 7.5 d)
117	Increase nutrient addition rate (HRT 7.5 d)	
209		Addition of Na_2S (20 mL/d with 1 g/L)
308		Addition of Na_2S (10 mL/d with 1 g/L) + KH_2PO_4 10 mL/d with 0.8 g/L
341		Increase concentration of KH_2PO_4 to 8 g/L
370	End	
381		End

2.6. Microbial sequencing and analysis

DNA extraction was completed using the FastDNA Spin Kit for Soil (MPBiomedicals, Illkirch-Graffenstaden, France) with 2 mL of the liquid sample following the manufacturer's instructions, with the following modifications: step 7 (10 min centrifugation at 14,000 RCF), step 9 (10 min of matrix settling), and an additional cleaning step between steps 11 and 12 with humic acid. The same extraction kit was used for the carrier biofilm samples. Before following manufacturer's instructions, the following steps were performed: 1. add 978 μL of sodium phosphate buffer and 122 μL of microtubule buffer to a Lysing Matrix E Tube; 2. resuspend the solution in the Lysis Matrix E Tube and transfer all the contents to a 5 mL Eppendorf tube; 3. select a representative carrier from the sample and place into the 5 mL tube; 4. vortex continuously at low speed for 1 min; 5. remove the carrier from the 5 mL tube; and 6. transfer everything from the 5 mL tube back into the Lysing Matrix E tube, then continue from step 3 of the manufacturer's instructions. Sequencing libraries were prepared and generated by SciLifeLab, Stockholm, Sweden, using Illumina MiSeq (2x300 bp) targeting 16S rDNA as described previously (Westerholm et al., 2018). Adapters were removed from the paired-end reads using Cutadapt version 1.13 on the forward and reverse reads (GTGBCAGCMGCCGCGGTAA and GACTACHVGGGTATCTAATCC, respectively) and filtered based on quality and trimmed reads to 250 bp. The trimmed reads were processed using Division Amplicon Denoising Algorithm2 (DADA2) version 1.16.0 in RStudio running R version 4.3.1, as described by Westerholm et al. (2018), with forward and reverse reads truncated at positions 240 and 160, respectively. The SILVA reference database v. 138 was used for microbial classification. The data was organized using phyloseq v1.44.0 (McMurdie & Holmes, 2013) in a single data object. The DADA2 analysis was completed on the UPPMAX high-performance computing cluster. The single data object created was visualized in R Studio 2024.09.1 (RStudio Team, 2021) running R v4.4.1. The following R packages were installed for the visualization of the microbial data: ggplot v3.5.1, data.table v1.15.4, plotly v4.10.4, lattice v0.22.6, permute v0.9.7, vegan v2.6.6.1, readxl v1.4.3, plyr v1.8.9, grid v4.4.1 and ggtext v0.1.2. Weighted principal coordinate analysis (PCoA) was calculated using the UniFrac method (Lozupone & Knight, 2005) based on the maximum-likelihood phylogenetic tree generated with FastTree (v2.1.11) (options –nt, –gtr, –gamma were used) using an alignment of all the amplicon sequence variants (ASV) with MAFFT (v7.526). To determine potential species similarity, the ASVs were submitted to the Basic Local Alignment Search Tool (BLAST) algorithm provided by the National Center for Biotechnology Information (NCBI). Raw sequence data have been deposited in NCBI PRJNA1268893.

To quantify the total amount of methanogens, a qPCR was performed using the primers mcrA-rev (CGTTCATBGCGTAGTTVGGRTAGT) and mcrA-F3 (CTTGAARMTCACTTCGGTGGWTC) (Steinberg & Regan, 2008; Cisek et al., 2022). The fragment amplification was completed using Thermo Fisher Scientific QuantStudio 5 programed to run at 98 °C/10 s, 56 °C/30 s, 72 °C/30 s, 35 cycles. For the construction of DNA standards for methanogens, the methanogens were amplified from environmental manure samples using primers mcrA-rev and mcrA-F3. The mcrA genes amplified were PCR purified using Qiagen (QIAquick PCR Purification Kit) and cloned into the pGEM-T Easy Vector System (Promega) and transformed into competent *Escherichia coli* cells following the manufacturer's instructions. Plasmids were extracted using QIAprep spin miniprep kit (Qiagen, Hilden, Germany) and sent to Macrogen for sequencing using Macrogen's standard primers M13F-pUC

(−40) and M13R-pUC (−40).

2.7. Calculations

The average inflow-based hydraulic retention time of the nutrient media was calculated based on the addition of fresh nutrient medium V_M (L/d) to the reactor and the total liquid volume V_L in the reactor (1 L), as follows:

$$HRT = \frac{V_L}{V_M} \quad (1)$$

The methane evolution rate (MER) was calculated as shown in Eq. (2). Here, F_{out} (L/(L_{pbv}·d)) is defined as the total normalized product gas flow rate (1013.15 mbar, 273.15 K) including moisture and c_{CH4} is the CH_4 composition in the product gas.

$$MER = F_{out} * c_{CH4} \quad (2)$$

The conversion rate (%) of H_2 and CO was respectively calculated according to Eq. (3), where F_i *in* is the normalized flow rate of the specific gas compartment in the inlet gas (L/(L_{pbv}·d)) and F_i *out* is the normalized flow rate of it in the product gas at the outlet of the TBR.

$$conversionrate = \frac{F_i in - F_i out}{F_i in} * 100 \quad (3)$$

The inflow-based gas retention Time (GRT) was defined as the average time for the gas to stay in the packed bed volume without conversion of the gases according to Eq. (4), where V_{pbv} is the active packed bed reactor volume (mL), and F_{in} is the total normalized inflowing gas load (mL/h).

$$GRT = \frac{V_{pbv}}{F_{in}} \quad (4)$$

3. Results

3.1. The effect of nutrient media on process parameters

The results in this section are described based on the operational periods for each reactor (Table 1). As a result of the major operational guideline to maintain high H_2 and CO conversion rates, no periods of VFA accumulation (< 0.6 g/L) were observed during the entire operation of 370 and 381 days for TBR1 and TBR2, respectively (Fig. S2a; supplementary material).

3.1.1. Start-up – without nutrient medium addition

The operation process during the start-up period was identical for TBR1 and TBR2. Straight after inoculation with the digestate mixture, syngas was applied to the reactors. During the first 62 days, the syngas load was increased stepwise (usually every 7–10 days), depending on H_2 and CO conversion, up to a final syngas load of ca. 5.3 L/(L_{pbv}·d) (GRT 4.5 h; Fig. 2a and 3a). This resulted in a MER of ca. 0.9 L/(L_{pbv}·d), while conversion rates for both H_2 and CO (Fig. 2b and 3b) were very high (>99 %). In both TBRs, PO_4^{3-} declined from 160 mg/L to 35–70 mg/L, whereas NH_4^+ remained stable at around 400 mg/L in TBR1 and slightly increased to 500–600 mg/L in TBR2 (Fig. 2c and 3c). The alkalinity declined from 4000 to 3000 mg $CaCO_3$/L, and the pH dropped from 8.5 to around 7.3 in both reactors (Fig. 2e and 3e). Furthermore, the concentration of SO_4^{2-} decreased from 385 to 90–95 mg/L (Fig. 2d and 3d), and H_2S in product gas declined below 10 ppm, indicating reduced bioavailability of sulfur in the form of sulfide (S^{2-}) in both reactors.

3.1.2. Trickle-bed reactor 1 – Digestate as nutrient medium

3.1.2.1. Hydraulic Retention Time 15 d. After the start-up phase, diluted digestate was added to TBR1 from day 62, at an HRT of 15 d, i.e., with the addition of 65–70 ml nutrient medium/d. The decreasing SO_4^{2-} concentration observed during the start-up phase was stabilized at ca. 100 mg/L, and the H_2S level in the product gas stabilized at ca. 5–10 ppm (Fig. 2d) during the continuous addition of digestate. The syngas load was increased stepwise between day 60 and day 100 (Fig. 2a) up to 19 L/(L_{pbv}·d) (GRT 1.25 h), while conversion rates for H_2 and CO were

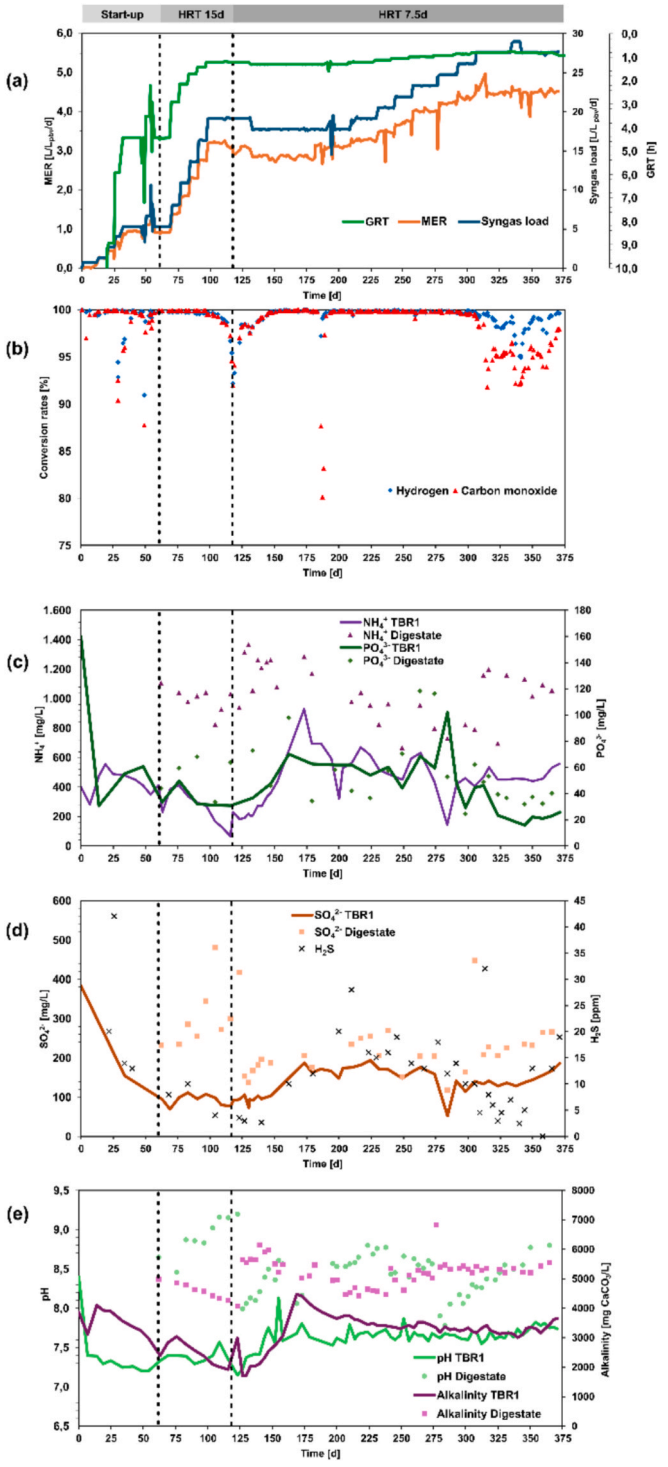

Fig. 2. TBR1: (a) Development of syngas load, gas retention time (GRT)* and Methane Evolution Rate (MER), (b) H_2 and CO conversion rates, (c) NH_4^+ and PO_4^{3-} levels of TBR liquid and digestate, (d) SO_4^{2-} levels of TBR liquid and digestate, and H_2S concentration in product gas, and (e) pH and alkalinity of TBR liquid and digestate. *TBR1 started with GRT of 35d which is beyond the scale.

kept close to 100 %. During periods of full conversion of H_2 and CO, the product gas of the TBR was comprised of 29 % CH_4 and 48 % CO2 with 22 % N_2 (Fig. S2b; SM). On day 100, MER was ca. 3.2 L/(L_{pbv}·d) (Fig. 2a). A slight drop in H_2 and CO conversion rates was detected from day 100. The conversion rates for H_2 and CO declined simultaneously (Fig. 2b) and in parallel with decreasing NH_4^+ levels from 230 mg/L on day 62 to 65 mg/L on day 116 (Fig. 2c). This was alongside a decrease in alkalinity to 1900 mg $CaCO_3$/L on day 116 with pH stability between 7.3–7.5. To overcome this negative trend, the addition of the nutrient medium was increased by 100 %, decreasing the HRT from 15 to 7.5 d on day 117.

3.1.2.2. Hydraulic Retention Time 7.5 d. The increased addition of the nutrient medium led to increasing concentrations of NH_4^+, SO_4^{2-} and PO_4^{3-} and the conversion rates of H_2 and CO increased from 92-95 % on day 117 to nearly full conversion around day 145 (Fig. 2b). The concentrations of NH_4^+ increased to > 900 mg/L on day 174 followed by a decrease, finally reaching a steady state between 400–600 mg/L until the end of the trial on day 371 (Fig. 2c). Furthermore, PO_4^{3-} concentrations rose from 35 to 70 mg/L on day 161, followed by a steady state until day 285 and a declining trend down to 15 mg/L on day 350, likely connected to increased syngas loads at this time. At HRT 7.5 d, stable alkalinity and SO_4^{2-} concentrations were observed, which were above 3000 mg $CaCO_3$/L and 150 mg/L, respectively. H_2S concentrations in the product gas were usually between 5 and 30 ppm (Fig. 2d), indicating sufficient S supply with the liquid medium.

On day 210, the strategy of stepwise increasing the syngas load was continued up to the maximum MER of 4.5 L/(L_{pbv}·d) on day 306 (Fig. 2a). The corresponding syngas load was 27–28 L/(L_{pbv}·d) (GRT 0.9 h) and both H_2 and CO were converted by > 99 %. With a further increase of syngas load, the conversion rates began to drop to 95–99 % and 95–97 % for H_2 and CO, respectively. During this time, the MER remained constant at approximately 4.5 L/(L_{pbv}·d). Thus, syngas load above 28 L/(L_{pbv}·d) (GRT 0.8 h) did not lead to higher MER, but rather to declining H_2 and CO conversion rates. In general, the potential contribution of CH_4 in the diluted digestate was assessed to be negligible. The maximum daily production based on the highest supply rate (HRT 7.5 d) and residual methane potential (20 ml/g VS) only resulted in ca. 2 mL CH_4/d when the daily CH_4 production was above 15 L/d.

3.1.3. Trickle-bed reactor 2 – Reject water as nutrient medium

3.1.3.1. Hydraulic Retention Time 15 d. The addition of reject water as nutrient medium (HRT 15 d) started simultaneously with the addition of digestate to TBR1 on day 62. Identically to TBR1, the syngas load was increased stepwise up to ca. 19–20 L/(L_{pbv}·d) (GRT 1.25 h) within this period (Fig. 3a), reaching a maximum MER of ca. 3.1 L/(L_{pbv}·d) on day 100 with conversion rates of 97 % and > 99 % for H_2 and CO, respectively. As for TBR1 and during periods of full conversion of H_2 and CO, the product gas of the TBR was comprised of 29 % CH_4 and 48 % CO2 with 22 % N_2 (Fig. S2c; SM). There was a clear decreasing trend in macronutrient concentrations, which negatively affected the H_2 and CO conversion rates. NH_4^+ concentration decreased from 500 to 90 mg/L, and PO_4^{3-} declined from 75 to 10 mg/L within this period (Fig. 3c). Besides the drop in alkalinity from 3000 to 1000 mg $CaCO_3$/L (Fig. 3e), a decline in H_2S in the product gas was observed. From day 100 onwards, no H_2S was detected in the product gas, while the H_2 conversion rate was reduced to ca. 86 %. In contrast to TBR1, CO conversion changed very little at that time, remaining stable above 98 % (Fig. 3b). The low concentration of macronutrients and, additionally, the absence of H_2S indicated the need for an increase in nutrient feeding (in line with TBR1). On day 109, the nutrient medium addition was doubled to ca. 133 mL/d, which reduced HRT from 15 d to 7.5 d.

3.1.3.2. Hydraulic Retention Time 7.5 d. The increased supply of nutrients at the beginning of this period did not have an immediate effect on the conversion of H_2 (low rates between 83–91 %) in comparison to TBR1. To restore the H_2 conversion rates and avoid VFA accumulation, the syngas load was stepwise reduced from 19.5 L/(L_{pbv}·d) on day 117 to 8 L/(L_{pbv}·d) (GRT 3 h) on day 130. This measure finally led to

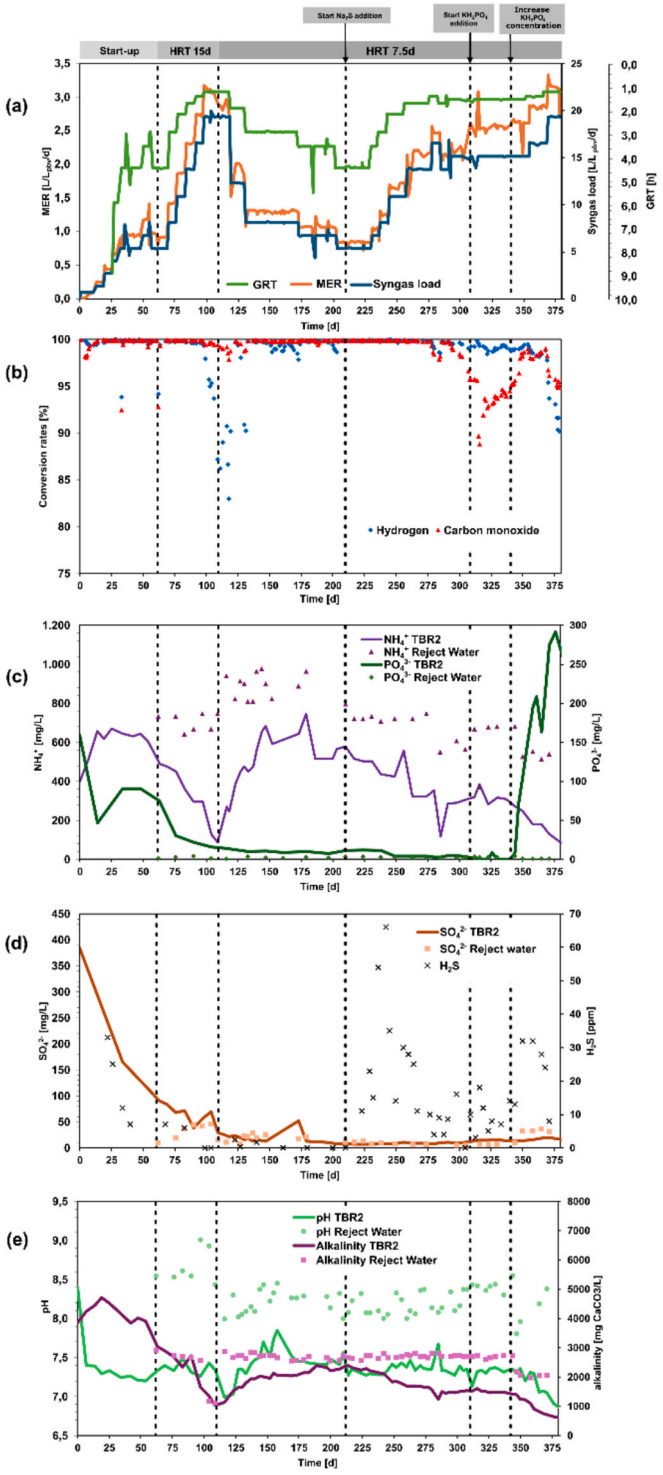

Fig. 3. TBR2: (a) Development of syngas load, gas retention time (GRT)* and Methane Evolution Rate (MER), (b) H_2 and CO conversion rates, (c) NH_4^+ and PO_4^{3-} levels of TBR liquid and reject water, (d) SO_4^{2-} levels of TBR liquid and reject water, and H_2S concentration in product gas, and (e) pH and alkalinity of TBR liquid and reject water *TBR2 started with GRT of 35d which is beyond the scale.

improved conversion rates of both H_2 and CO. Up to day 150 the concentration of NH_4^+ recovered and reached 600–700 mg/L (Fig. 3c). However, SO_4^{2-} and PO_4^{3-} remained at low levels despite the increased nutrient solution addition in this period, likely because the reject water itself was very low in SO_4^{2-} and PO_4^{3-} (Fig. 3c and 3d). From day 160 onwards, no H_2S was detected in the product gas and H_2 conversion rates dropped again, as seen earlier at HRT 15 d, leading to another decrease in syngas load to 6–7 L/(L_{pbv}·d) (GRT 3.6 h) with a corresponding maximum MER of 1.1 L/(L_{pbv}·d) from day 175 onwards (Fig. 3a). Based on the very low concentration of SO_4^{2-} and PO_4^{3-}, the decision to add supplemental nutrients in the next period was taken.

3.1.3.3. Hydraulic Retention Time 7.5 d with Na_2S addition. The addition of 20 ml Na_2S solution (1 g/L) per day started on day 209 to mitigate declining H_2 and CO conversion rates, and an immediate response by the system was observed. H_2S was detectable at levels of 10–30 ppm in the product gas, and the conversion rates of H_2 and CO were close to 100 %, allowing a stepwise increase of the syngas load. From day 250 onwards, the Na_2S addition was reduced to 10 mL/d because H_2S concentrations above 30 ppm in the product gas indicated overfeeding (Fig. 3d and Table 1). Between day 209 and day 308, NH_4^+ decreased from 580 to 300 mg/L, while the added reject water also had lower NH_4^+ levels (Fig. 3c). Syngas loads were increased up to 14–15 L/(L_{pbv}·d) (GRT 1.6 h) around day 300 (Fig. 3a). With this syngas load, the conversion rates began to drop slightly to 98 % and 96 % for H_2 and CO, respectively (Fig. 3b), and MER increased to around 2.5 L/(L_{pbv}·d) at the end of that period. Interestingly, the CO conversion was affected more than the H_2 conversion, which differed from the declining conversion rates observed between days 100 and 125, where only the H_2 conversion was affected. In comparison to TBR1, the MER and H_2 and CO conversion rates were lower, and the low PO_4^{3-} concentration (2–4 mg/L) in the liquid phase of TBR2 indicated that P could be a limiting factor.

3.1.3.4. Hydraulic Retention Time 7.5 d with Na_2S and KH_2PO_4 addition. On day 308, a daily addition of 10 ml KH_2PO_4 solution (0.8 g/L) started as a second supplement besides Na_2S. However, the concentration of PO_4^{3-} in TBR2 liquid did not increase and the CO conversion rates stayed low (88–94 %) (Fig. 3b). MERs did not exceed levels above 2.6 L/(L_{pbv}·d) (Fig. 3a). From day 341, the concentration of the KH_2PO_4 solution was increased ten-times (8 g/L) and PO_4^{3-} levels in the nutrient liquid raised from 0.5 to more than 250 mg/L at the end of the trial (day 381). Consequently, increasing CO conversion rates were observed, and syngas loads were increased above 16 L/(L_{pbv}·d) (GRT 1.5 h). At this load, MER was 2.9 L/(L_{pbv}·d) with still proper H_2 and CO conversion rates (>98 %) (Fig. 3a and 3b). Between day 341 and 381, the alkalinity declined from 1200 to 600 mg $CaCO_3$/L, pH decreased from 7.3 to 6.9 (Fig. 3e) and NH_4^+ decreased from 300 to 100 mg/L (Fig. 3c). A final approach in increasing syngas loads up to 19 L/(L_{pbv}·d) (GRT 1.2 h), was responded with decreasing conversion rates (90–95 %) of both H_2 and CO with a corresponding maximum MER of 3.1 L/(L_{pbv}·d) (Fig. 3a and b).

3.2. Effect of nutrient media on microbial community development

The analysis of the microbial community composition in the liquid phase and on the carriers showed that there were no obvious differences between TBR1 and TBR2, despite the differences in syngas load, H_2 and CO conversion rates, and MER. The communities in the liquid phase were slightly different in the early phase of operation, but over time each reactor gradually transformed towards similar compositions (Fig. 4). The difference between the starting communities and the final communities in each reactor are mostly explained by principal coordinate 1, which accounts for 62.5 % of the variation.

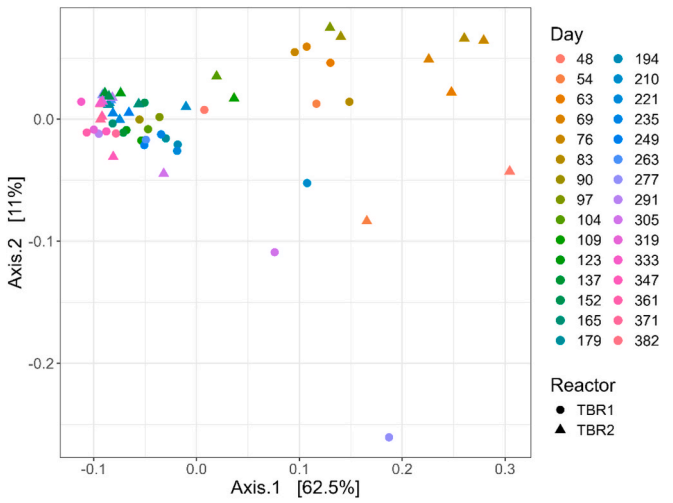

Fig. 4. Weighted principal coordinates analysis plot highlighting the microbial community development in the liquid phases of TBR1 (circles) and TBR2 (triangles) with colors indicating the sampling day.

3.2.1. Archaea

The methanogen belonging to *Methanothermobacter* was the primary methanogen in both TBR1 and TBR2 (Fig. 5). The NCBI BLAST result of the amplicon sequence variance (ASV) revealed the methanogen to be *Methanothermobacter marburgensis* with 100 % query coverage and 100 % identity. The relative abundance (RA) of this ASV gradually increased towards the end of the operation in both TBR1 and TBR2 (Fig. 5). In TBR1, the initial level was 17–39 %, while the RA was 69–92 % at the end of the operation (Tab. S3; SM). In TBR2, the corresponding values were 1–15 % and 78–84 %, respectively (Fig. 5, Tab. S3; SM). Alongside *Methanothermobacter* in TBR1, two additional methanogens, one belonging to *Methanobacterium* and one representing an unknown genus of *Methanobacteriales*, were present throughout the operation at comparably lower RA (1–5 %) (Fig. 5, Tab. S3; SM). The same methanogens were initially seen in TBR2 at similar RA (1–12 %) but disappeared (<1%) after 210 days of operation. The ASV for *Methanobacterium* was *Methanobacterium formicicum* at 100 % query coverage and 100 % identity. The ASV for *Methanobacteriales* was matched to three different species of *Methanothermobacter*, *M. marburgensis*, *M. thermautotrophicus*, and *M. defluvii*, all with 100 % query coverage and 98 % identity. The qPCR analysis of methanogens in the liquid phase revealed that the quantity of the methanogens was initially higher in TBR2 between days 83–123 (Fig. 5, SM). Over time, the abundance of the total methanogens equaled the same amount.

The methanogenic community on the carriers from each reactor, independent of their reactor position, reflected a similar composition to that of the liquid phase, with some minor differences (Fig. S4; SM). The methanogen ASVs on the carriers in TBR1 belonged to the dominating *Methanothermobacter* (5–83 %); *Methanobacterium* was also detected (1–2.8 %) (Fig. S4; SM). However, a small percentage of *Methanosarcina* (1–7 %) (Fig. S4; SM) was detected on the carriers. TBR2 primarily had *Methanothermobacter* (25–77 %) and *Methanobacterium* (1–9 %), the former being the dominant methanogen (Tab. S3; SM).

The qPCR analysis showed that the abundance of the total methanogens in the liquid fluctuated between $1.8x10^5$ to $5.8x10^5$ gene copies/L in TBR1 and $6.4x10^4$ to $1.2x10^6$ gene copies/L in TBR2. The abundance of the total methanogens near the end of the operation of both reactors was similar (Fig. S5; SM). There was a major increase of methanogens in TBR2 compared to TBR1 (Fig. S5; SM) within the operational period with HRT 15 d, when the syngas load was stepwise increased in TBR2 (Fig. 3a). Afterwards, when the syngas load was again decreased, the abundance dropped below that of TBR1 (Fig. S5; SM). Another dip in methanogenic abundance in TBR2 was seen around the

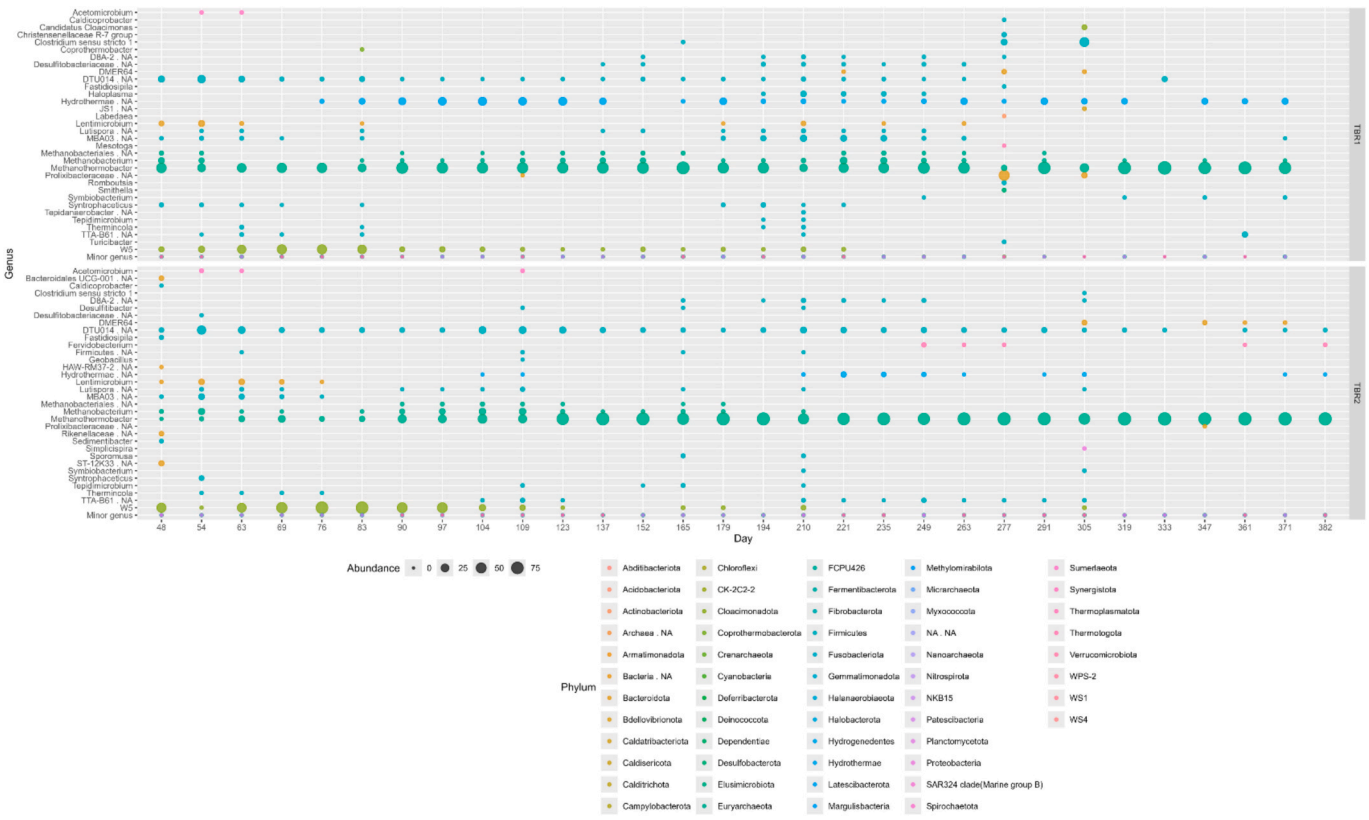

Fig. 5. Bubble plot of the relative abundance of the microbial community composition in the liquid phase of TBR1 (top plot) and TBR2 (bottom plot). The x-axis indicates the day of the sampling. The phylum level is depicted by the color of the bubbles and the genus is presented on the y-axis.

same time as the second decrease in the syngas load. However, the level increased to a similar level in TBR1 from day 250 after the addition of Na_2S into TBR2 on day 209.

3.2.2. Bacteria

The bacterial communities in the liquid phase of TBR1 and TBR2 also showed similar structures (Fig. 5). Both reactors showed a relatively high presence of an ASV belonging to the genus *W5* at the beginning of the operation, but this species gradually decreased over time. A similarly decreasing trend was seen for an ASV belonging to the order *DTU014*, but with some slight differences between the reactors at the end of the operation, with a higher RA in TBR2. This ASV was similar to an unidentified thermophilic *Eubacterium ST12* with 100 % query coverage and 97 % identity. A clear difference was seen between the reactors for an ASV belonging to the phylum *Hydrothermae*, which was recovered in TBR1 throughout many of the days of operation but only during a short period in TBR2. The BLAST result of this ASV revealed its closest relative to be *Thermotogales* sp. SRI-15 with 100 % query coverage and 96 % identity. Another ASV appeared mainly in TBR1 and shared 95 % identity in 100 % query coverage to *Syntrophaceticus schinkii*. An ASV belonging to *MBA03* was seen during the early phase of operation in both TBR1 and TBR2, whereafter it disappeared from TBR2 while fluctuating at low RA throughout the entire operation of TBR1.

In the carrier communities, the composition shared similarities to the liquid phase of the reactors. The abundance was slightly different between levels in the reactor, but with no consistency between reactors and sampling occasions. The carriers in TBR1 showed the presence of *DTU014* (2–10 %), *Hydrothermae* (1–40 %), *MBA03* (1–4 %), *Syntrophaceticus* (1–7 %), and *W5* (1–72 %) (Tab. S3 and Fig. S4; SM). On TBR2 carriers, similar groups of microbes were identified, including *DTU014* (1–9 %), *Hydrothermae* (2–10 %), *MBA03* (1 %), *Syntrophaceticus* (1 %), and *W5* (2–4 %). Additionally, an ASV belonging to the genus *Thermacetogenium* was recovered in TBR1 (6 %), which was BLASTed to be 99.2 % similar to Thermacetogenium phaeum over 100 % query coverage.

4. Discussion

4.1. The effect of nutrient media composition on syngas biomethanation

Among macronutrients, NH_4^+ is a crucial nutrient, especially for methanogens (protein synthesis, enzymatic activity), contributing to buffer capacity and maintaining a stable pH (Dupnock & Deshusses, 2019; Kamravamanesh et al., 2023). The reported minimum NH_4^+ levels vary for TBR biomethanation systems, ranging between 60 mg/L (Thema et al., 2021) and 1000 mg/L (Dupnock & Deshusses, 2019). For TBR1, utilizing digestate as the nutrient medium, low NH_4^+ concentrations of 65 mg/L were analyzed at the end of the operation period with HRT 15 d and were most likely responsible for declining H_2 and CO conversion rates (Fig. 2b). Due to increased nutrient medium addition (HRT 7.5 d), suggested NH_4^+ levels above 400 mg/L (Feickert Fenske et al., 2023a) were ensured to maintain high CH_4 productivity in combination with nearly complete conversion of H_2 and CO in TBR1.

For TBR2, a decline in NH_4^+ and SO_4^{2-} could be observed at HRT 15 d. Additionally, H_2S was no longer detected in the product gas towards the end of this period. Shortages of N and S were the most likely reasons for the observed decreasing conversion rates. From day 110 to 125, the H_2 conversion rate decreased to 82–95 %, while the CO conversion remained over 98 %. The lack of available S likely inhibited the hydrogenotrophic methanogens, causing an accumulation of H_2 in TBR2. During the same period, TBR1 showed a decrease in the conversion rate of both H_2 and CO to 92 % but only with a decreased concentration of NH_4^+. The increased inflow of reject water (HRT 7.5 d) had a positive impact on the NH_4^+ levels in the reactor liquid, which increased from day 109 onwards. The rising NH_4^+ concentration was also influenced by declining syngas loads, which were drastically reduced from 20 to 6 L/(L_{pbv}·d) (Fig. 3a) to maintain high H_2 and CO conversion

rates, resulting in lower microbial nutrient consumption. With increasing syngas loads starting around day 230, the trend in NH_4^+ concentration decreased again, maintaining lower concentrations (100–350 mg/L) after day 280. This indicates that the HRT should be further decreased to generally ensure NH_4^+ levels of around 400 mg/L.

Phosphorus is essential for methanogenesis (i.e., ATP synthesis via the acetyl-CoA pathway), ensuring an optimal C:N:P relation for methanogens of 100:3:1 (Gerardi, 2003) with the minimum concentration reported to be 1–2 mg/L (Gu et al., 2022). Severe inhibition of methanogenesis is documented at a PO_4^{3-} concentration above 2300 mg/L (Lackner et al., 2020). In TBR1, no PO_4^{3-} shortages were observed because its concentration varied between 20–100 mg/L throughout the entire operation. In TBR2, on the other hand, PO_4^{3-} was comparatively low, with concentrations below 10 mg/L from day 240 onwards and remaining at concentrations below 2 mg/L between days 312 and 343. A decrease in H_2 and CO conversion rate, starting on day 275, may be associated with limited PO_4^{3-} availability. The PO_4^{3-} concentration of the utilized reject water varied between 1–4 mg/L throughout the experiment (Fig. 3c), thus, likely not providing enough essential P. During the first phase of adding a KH_2PO_4 solution (0.8 g/L), the PO_4^{3-} levels in the TBR2 liquid did not change and remained below 1 mg/L. Still, the conversion rates of CO improved, suggesting a positive effect on PO_4^{3-} availability and microbial activity. However, after a ten-fold increase in the amount of PO_4^{3-} added to TBR2 from day 341 onwards, the PO_4^{3-} concentration in the reactor liquid increased rapidly within a short time. It can be assumed that this had an inhibitory effect on the H_2 and CO conversion performance in line with reports from Mancipe-Jiménez et al. (2017), who reported a sudden increase from 3.3 to 33 mg P/L (101.2 mg/L of PO_4^{3-}) in phosphorus concentration in anaerobic waste treatment. This imbalanced the equilibrium between bacteria and methanogens, causing a decrease in methanogenic activity. Concerning the present study, this explains why TBR2 did not achieve the same performance as TBR1 despite S and P supplementation. Additionally, the observed decline in H_2 and CO conversion rates from day 368 to 381 can be directly linked to an increased syngas load (16.5 to 19 L/(L_{pbv}·d)). Nevertheless, in future P-optimizing studies of biomethanation, the application of supplementary P should be applied carefully. However, based on our results, the PO_4^{3-} concentration in the TBR liquid should be above 20 mg/L to maintain high conversion of H_2 and CO.

The addition of Na_2S to TBR2 raised the availability of S_2^- in the reactor and, thus, hydrogenotrophic methanogens were able to metabolize H_2 and CO_2 to a higher degree, which was in line with several previous studies (Rachbauer et al., 2016; Strübing et al., 2017; Asimakopoulos et al., 2019; Dupnock & Deshusses, 2019; Thema et al., 2021). S^{2-} is essential for methanogens, more specifically for the biosynthesis of coenzymes involved in the final step of methanogenesis (methyl-CoM reductase) and for the biosynthesis of Fe-S clusters, which are found in other enzymes involved in H_2 oxidation/ CO_2 reduction and electron transport. Under S^{2-} shortages, the biomethanation performance is inhibited (Thema et al., 2021) but can recover quickly when the S_2^- concentration is above 0.02 mM (6.4 mg/L) (Strübing et al., 2017). However, when S^{2-} is in excess, it can precipitate trace elements (i.e. Fe, Ni and Co), which are essential for many enzymes and for microbial activity. Therefore, the addition of Na_2S should be used with caution to circumvent process failure. It can be recommended to follow the H_2S concentration in the product gas maintaining levels between 5–30 ppm.

In contrast to the present study, Kamravamanesh et al. (2023) did not see macronutrient limitation for the reject water per se, but still proposed the addition of trace elements to maintain high H_2 conversion rates. The addition of trace elements was shown to improve H_2 and CO conversion and CH_4 productivity when using digestate as a nutrient medium (Goonesekera et al., 2024). However, information about minimum concentrations of trace elements is scarce and varies among the available literature. Iron is of great importance for methanogens, and sufficient Fe levels are reported to be above 1.5 or 2 mg/L in the nutrient liquid (Dupnock & Deshusses, 2019; Ashraf et al., 2021). In the present study, the Fe concentration of the diluted digestate was 14 mg/L (Tab. S1; SM), indicating a sufficient supply of this specific element, whereas in reject water, only 4 mg/L were analysed, which may be a limiting factor. However, for other important trace elements such as Co, Mo, Ni, and Zn, the concentrations in the digestate were considerably higher compared to the reject water (Tab. S1; SM), making it a potent alternative to defined nutrient media. Still, it is unclear to what extent those elements are present in a bioavailable form to be metabolized by the microbial community. For future research, micronutrients should be considered as an important threshold for continuous syngas biomethanation systems.

4.2. The performance of hydrogen and carbon monoxide conversion and methane production using trickle-bed reactors

Studies of biomethanation using only H_2 and CO_2 have achieved MERs between 1 and 15 L/(L_{pbv}·d), depending on several operational parameters, such as temperature, H_2:CO_2 ratio, and applied pressure (Burkhardt & Busch, 2013; Strübing et al., 2017; Porte et al., 2019; Feickert Fenske et al., 2023a). However, MERs for syngas biomethanation are expected to be lower for stochiometric reasons, as the presence of CO potentially limits the production of CH_4 (Sancho Navarro et al., 2016). In the present study, TBR1 showed a maximum MER of 4.5 L/(L_{pbv}·d), maintaining H_2 and CO conversion rates above 95 % during long-term (ca. one year) experimentation. To the best knowledge of the authors, there are currently only two studies of syngas biomethanation using TBR that show higher MERs. Asimakopoulos et al. (2021) operated a 5 L TBR under thermophilic conditions with a defined basal nutrient medium (HRT 8 d) and achieved a MER of up to 9.5 L/(L_{pbv}·d) with conversion rates of 97 % and 76 % for H_2 and CO, respectively. Goonesekera et al. (2024) documented a maximum MER of 5.3 L/(L_{pbv}·d) using digestate (HRT 20 d) with supplementary trace elements using a thermophilic 1 L TBR and achieving "full H_2 and CO conversion". Without the addition of trace elements, the latter study achieved slightly lower MERs (4.3 L/(L_{pbv}·d)) compared to the present study, maintaining lower conversion rates for H_2 (<90 %) and CO (<80 %). Furthermore, Asimakopoulos et al. (2021) and Goonesekera et al. (2024) used a syngas composition with higher H_2 shares (45 and 65 %, respectively) and lower shares of CO (20 and 17 %, respectively) and CO_2 (25 and 13 %, respectively) in comparison to the present study (40 % H_2, 30 % CO, 20 % CO_2 and 10 % N_2). Additionally, other than using a defined basal medium as the nutrient source, Asimakopoulos et al. (2021) applied a pH control, and the liquid recirculation was continuous. Another major difference from the present study was the choice of carrier material. The specific surface of the carriers within our study was 500 m^2/m^3, which was identical to the one in Goonesekera et al. (2024), whereas Asimakopoulos et al. (2021) used a packing material with 800 m^2/m^3.

Regarding studies using digestate as a nutrient medium without supplementary nutrient addition, Andreides et al. (2022b) documented a MER of 2.1 L/(L_{pbv}·d) using a 1 L TBR under thermophilic conditions when investigating the influence of temperature for syngas biomethanation at an HRT of 6 d. With only CO as the sole carbon source, Ali et al. (2024) achieved a MER of 0.99 L/(L_{pbv}·d), continuously utilising digestate within a 0.7 L TBR.

In TBR1, from day 300 onwards, the conversion rates for H_2 and CO decreased to 95–99 % and 92–97 %, respectively. This was likely caused by reaching the maximum syngas load capacity during prevailing conditions. Limiting factors concerning macronutrient levels could not be determined because no shortages in the trickling liquid or lack of sulfur (i.e., H_2S in the product gas) were observed at that time. The decline in conversion rates was most likely connected to low gas retention times in the reactor caused by gas–liquid mass transfer limitations (Asimakopoulos et al., 2019; Dupnock & Deshusses, 2019; Jensen et al., 2021). At syngas loads of 27–30 L/(L_{pbv}·d), the gaseous retention time in the TBR was between 0.8 to 0.9 h, and in combination with the specific area of the chosen carriers, it might have limited the gas–liquid mass

transfer. Consequently, higher syngas loads at the end of this final period did not result in higher CH_4 productivity but only in lower H_2 and CO conversion rates. Still, the addition of trace elements as done by Goonesekera et al. (2024), seems to be a reasonable option to further increase MERs while maintaining high conversion rates for digestate-driven syngas biomethanation systems.

In comparison to TBR1, the assessment of reject water as a nutrient medium in TBR2 was characterized by lower MERs during periods of sole reject water feeding (maximum MER up to 1 $L/(L_{pbv}{\cdot}d)$). This aligns with previous findings of Cheng et al. (2022), achieving a MER of 1 $L/(L_{pbv}{\cdot}d)$ during continuous syngas biomethanation in a mesophilic 35 L TBR. Under thermophilic conditions with H_2 and CO_2 as the only gaseous substrate, another study observed MERs of up to 2.6 $L/(L_{pbv}{\cdot}d)$ using trace element-modified reject water as a nutrient medium in an 8.3 L TBR (Kamravamanesh et al., 2023). In the present study, a higher MER of 3.1 $L/(L_{pbv}{\cdot}d)$ and H_2 and CO conversion rates above 91 % were achieved for reject water with supplements for S and P. To our knowledge, this is the highest MER observed for biomethanation using reject water as a nutrient medium. However, to reach even higher MER while maintaining H_2 and CO conversion rates in the same order of magnitude as digestate, additional supplements such as trace elements will be required, as shown in Kamravamanesh et al. (2023).

4.3. Microbial community development

The syngas biomethanation process relies on a mixed microbial consortium involving both bacteria and archaea. Key groups in the process include hydrogenotrophic and acetoclastic methanogens, acetogens, and SAOBs, which were all found in the present study. Interestingly, even though the reactors showed differences in performance depending on the nutrient source, no major differences were seen in the community structure or methanogenic abundance in the liquid phase (Fig. 5) or on the carriers (Fig. S4; SM), suggesting that the difference in MER between TBR1 and TBR2 was mainly related to the activity of the communities and not to the community members per se.

In line with other studies on thermophilic syngas biomethanation, CH_4 was mostly produced by hydrogenotrophic methanogens (Asimakopoulos et al., 2019; Goonesekera et al., 2024). *Methanothermobacter* was the dominant methanogen, followed by *Methanobacterium* in both the liquid phases and on the carriers, and both groups have been seen to dominate the archaeal community in biomethanation systems with both H_2/CO_2 and syngas (Grimalt-Alemany et al., 2019; Goonesekera et al., 2024). The *Methanothermobacter* ASV was closely identified as *M. marburgensis*, which has been shown to effectively utilize both syngas and even to grow on CO as the sole substrate (Diender et al., 2016). While *M. thermautotrophicus* is typically the dominant methanogen in thermophilic biomethanation processes, its CO consumption can be limited at higher concentrations of CO, particularly without a carboxydotrophic partner, such as *Carboxydothermus hydrogenoformans* (Diender et al., 2016). However, while *M. marburgensis* prefers to use H_2/CO_2, this methanogen exhibits better CO utilization compared to *M. thermautotrophicus* (Diender et al., 2016), which likely explains its dominance in the presently investigated reactors.

Both reactors showed low levels of acetate or other VFAs during the whole period of operation (Fig. 2a, SM), suggesting that acetate was efficiently consumed. Acetate can be produced both by the conversion of CO or of H_2 and CO_2 via homoacetogenesis, which has been shown to be competitive with methanogenesis under some conditions, such as high gas load (Liu et al., 2016). Acetogens are also typically more tolerant to CO compared to methanogens, even those using CO (Alves et al., 2013). In addition, acetate can also be produced by fermenting bacteria growing on decaying biomass, as shown in several studies on biomethanation (Grimalt-Alemany et al., 2019; Laguillaumie et al., 2022). In the present study, only one known acetogen, genus *Sporomusa*, occasionally appeared in the liquid phase of both reactors, and no obvious acetogens were found on the carriers. However, several known heterotrophic acetate-producing microbial groups, such as *Acetomicrobium, Coprothermobacter,* and *Lentimicrobium*, were present in low abundance. These genera have been found before in syngas-fed processes (Luo et al., 2013; Li et al., 2021; Laguillaumie et al., 2022; Ali et al., 2024). Another potential acetate producer was represented by the ASV belonging to the candidatus phylum Hydrothermae, present only in TBR1 in both the liquid and on the carriers. This ASV is most closely identified with *Thermotogales* sp. *SRI-15*, which belongs to the order *Thermotogales*, is known to include thermophilic fermenting members producing acetate, CO_2, and H_2 (Reysenbach et al., 2001). Both reactors also initially showed a high abundance of an ASV belonging to *W5* (family *Cloacimonadaceae*), suggested to be a syntrophic propionate degrader producing acetate and H_2 as end products (Dyksma & Gallert, 2019). Interestingly, while acetate was likely formed, no acetate-consuming methanogens were identified in the liquid. However, *Methanosarcina* sp. was identified on the carriers in TBR1 but in lower relative abundance compared to *Methanothermobacter* sp. Species within *Methanosarcina* can use acetate, but some can also use H_2/CO_2 and CO (Rother et al., 2007; Luo et al., 2013), and thus their presence is not solely associated with acetate. In line with this, a previous study showed *Methanosarcina barkeri,* combined with *Methanothermobacter thermautotrophicus,* to be involved in CO biomethanation in a thermophilic CSTR reactor (Luo et al., 2013). Representatives in the genus *Methanosarcina* have been found before in both mesophilic and thermophilic syngas biomethanation processes (Aryal et al., 2021; Goonesekera et al., 2024). Acetate can also be consumed, in addition to methanogens, by syntrophic acetate-oxidizing bacteria (SAOB). In the present study, an ASV was closely related to a known SAOB (*S. schinkii*). This ASV was found in the liquid in both reactors, with higher abundances in TBR1. This SAOB has been observed previously in thermophilic biogas processes (Singh et al., 2023) and is suggested to play a key role in reaching efficient syngas conversion combined with *Methanothermobacter* (Ali et al., 2024). In addition, the carriers in TBR 1 indicated the presence of an ASV belonging to *Thermacetogenium*, matched to *Thermacetogenium phaeum*, known to convert acetate when partnered with hydrogenotrophic methanogens like *M. thermautotrophicus* (Hattori et al., 2005). However, *T. phaeum* can also take the role of an acetogen, converting H_2/CO_2 into acetate. Thus, its role in the present TBR reactors cannot be completely clarified. Moreover, two potential SAOBs were also present in both reactors, *DTU014* (Dyksma et al., 2020; Kamravamanesh et al., 2023) and family *MBA03* (Kamravamanesh et al., 2023), in both the liquid and carriers.

The finding of genus *Methanosarcina* only on the carriers was in line with a recent study by Goonesekera et al. (2024), who found this methanogen mainly present on carriers at the bottom of the TBR. The authors proposed a spatial specialisation in the carrier biofilm, with hydrogenotrophic methanogens in the top and acetate utilizers, methanogens, and SAOB at the bottom. Such spatial separation could not be determined in the present paper. Here, *Methanosarcina* was instead detected in the middle and at the top of the reactor, and SAOB and hydrogenotrophic methanogens were found at all levels. It is possible that these differences could be related to the counter-current operation of the TBRs in the present study, while the previous study by Goonesekera et al. (2024) used a co-current operation. However, to address differences and spatial distribution, more samples would be required. In the present study, the number of sampling occasions was limited, as removing carriers was challenging, and each sampling led to the introduction of oxygen and a reduction of syngas conversion.

4.4. Perspectives on syngas biomethanation

Considering the implementation of TBR syngas biomethanation on a production scale, there would be a synergy between establishing gasification of forest residues integrated with biogas plants, where digested residues can be utilized as nutrient media for TBRs. Furthermore, the combination of conventional biogas and biomethanised syngas will

increase the total gas flow, which can lead to a more cost-effective upgrading process to biomethane. The increased gas flow will further potentially facilitate the conversion to liquified biomethane. Digestates originating from well-functioning digestion processes likely contain all essential nutrients, as both AD and biomethanation are closely related microbial processes. Still, digestates likely must be processed (phase separation, dilution) before their utilisation as nutrient media. Reject water from dewatered digested sewage sludge shows lower concentrations of essential nutrients in general due to, for example, the use of polymers during dewatering. However, if a co-digestion plant and a WWTP are located close to each other, the option of using reject water for dilution of digestate instead of fresh water might be an option, as reject water generally contains relatively high concentrations of ammonium. This could facilitate the optimization of *N*-supply, reducing the nutrient addition rate needed and increasing process stability.

To further increase the MER with high syngas conversion using digestate as a nutrient source, further process parameters should be studied and optimized, including trace element supply, conditioning before use, carrier characteristics (e.g., liquid hold-up capacity), and liquid recirculation regimes.

5. Conclusions

Biomethanation of syngas was studied over a year in two identical trickle-bed reactors (TBRs) using diluted manure-based digestate and reject water from digested sewage sludge as non-defined nutrient sources, respectively. A maximum methane evolution rate (MER) of 4.5 $L/(L_{pbv}\cdot d)$ was achieved with digestate, maintaining H_2 and CO conversion rates above 95 %. In contrast, the specific reject water used in this study, characterized by low concentrations of phosphate and sulfate, resulted in only 1 $L/(L_{pbv}\cdot d)$, but supplementation with sulfur and phosphorus improved stability and conversion, reaching 3.1 $L/(L_{pbv}\cdot d)$ with H_2 and CO conversion over 91 %. These findings highlight the importance of key macronutrient availability for efficient syngas biomethanation, though further enhancement may require trace element supplementation. However, as digestate and reject water compositions might vary due to its origin and processing, these results should not be generalized beyond the specific nutrient media used in this study. Despite nutrient source differences, microbial community structures were similar in both reactors, with only minor variations due to the nutrient media. Methanogen abundance remained constant, suggesting MER differences were due to activity rather than community composition. The syngas-converting community was dominated by *Methanothermobacter* and included syntrophic acetate-oxidizing bacteria like *Syntrophaceticus* and *Thermacetogenium*.

CRediT authorship contribution statement

Florian Gabler: Writing – original draft, Visualization, Formal analysis, Data curation, Conceptualization. **George Cheng:** Writing – review & editing, Visualization, Formal analysis, Data curation. **Leticia Pizzul:** Writing – review & editing, Supervision, Funding acquisition, Conceptualization. **Anna Schnürer:** Writing – review & editing, Supervision, Funding acquisition, Conceptualization. **Åke Nordberg:** Writing – review & editing, Supervision, Funding acquisition, Conceptualization.

Declaration of competing interest

The authors declare that they have no known competing financial interests or personal relationships that could have appeared to influence the work reported in this paper.

Acknowledgments

This project was funded by the Swedish Energy Agency [149656-1] and Formas (2018-01341). The authors acknowledge Vasiliki Tsamadou for assistance with DNA extraction.

Appendix A. Supplementary data

Supplementary data to this article can be found online at https://doi.org/10.1016/j.biortech.2025.132893.

Data availability

The sequencing data generated and analyzed in this study are available in the NCBI repository under BioProject accession number PRJNA1268893.

References

Ali, R., Samadi, H., Yde, L., Ashraf, M.T., 2024. Carbon monoxide conversion by anaerobic microbiome in a thermophilic trickle bed reactor. Biochem. Eng. J. 212. https://doi.org/10.1016/j.bej.2024.109492.

Alves, J.I., Stams, A.J.M., Plugge, C.M., Madalena Alves, M., Sousa, D.Z., 2013. Enrichment of anaerobic syngas-converting bacteria from thermophilic bioreactor sludge. FEMS Microbiol. Ecol. 86 (3), 590–597. https://doi.org/10.1111/1574-6941.12185.

Andreides, D., Fliegerova, K.O., Pokorna, D., Zabranska, J., 2022a. Biological conversion of carbon monoxide and hydrogen by anaerobic culture: Prospect of anaerobic digestion and thermochemical processes combination. Biotechnol. Adv. 58, 107886. https://doi.org/10.1016/j.biotechadv.2021.107886.

Andreides, D., Lopez Marin, M.A., Zabranska, J., 2024. Selective syngas fermentation to acetate under acidic and psychrophilic conditions using mixed anaerobic culture. Bioresour. Technol. 394, 130235. https://doi.org/10.1016/j.biortech.2023.130235.

Andreides, D., Stransky, D., Bartackova, J., Pokorna, D., Zabranska, J., 2022b. Syngas biomethanation in countercurrent flow trickle-bed reactor operated under different temperature conditions. Renew. Energy 199, 1329–1335. https://doi.org/10.1016/j.renene.2022.09.072.

Aryal, N., Odde, M., Petersen, C.B., Ottosen, L.D.M. & Kofoed, M.V.W. (2021). Methane production from syngas using a trickle-bed reactor setup. *Bioresource Technology,* 333. https://doi.org/ARTN 12518310.1016/j.biortech.2021.125183.

Ashraf, M.T., Yde, L., Triolo, J.M., Wenzel, H., 2021. Optimizing the dosing and trickling of nutrient media for thermophilic biomethanation in a biotrickling filter. Biochem. Eng. J. 176. https://doi.org/10.1016/j.bej.2021.108220.

Asimakopoulos, K., Gavala, H.N., Skiadas, I.V., 2019. Biomethanation of Syngas by Enriched mixed Anaerobic Consortia in Trickle Bed Reactors. Waste Biomass Valoriz. 11 (2), 495–512. https://doi.org/10.1007/s12649-019-00649-2.

Asimakopoulos, K., Kaufmann-Elfang, M., Lundholm-Høffner, C., Rasmussen, N.B.K., Grimalt-Alemany, A., Gavala, H.N., Skiadas, I.V., 2021. Scale up study of a thermophilic trickle bed reactor performing syngas biomethanation. Appl. Energy 290. https://doi.org/10.1016/j.apenergy.2021.116771.

Burkhardt, M., Busch, G., 2013. Methanation of hydrogen and carbon dioxide. Appl. Energy 111, 74–79. https://doi.org/10.1016/j.apenergy.2013.04.080.

Burkhardt, M., Koschack, T., Busch, G., 2015. Biocatalytic methanation of hydrogen and carbon dioxide in an anaerobic three-phase system. Bioresour. Technol. 178, 330–333. https://doi.org/10.1016/j.biortech.2014.08.023.

Cheng, G., Gabler, F., Pizzul, L., Olsson, H., Nordberg, A., Schnurer, A., 2022. Microbial community development during syngas methanation in a trickle bed reactor with various nutrient sources. Appl. Microbiol. Biotechnol. 106 (13–16), 5317–5333. https://doi.org/10.1007/s00253-022-12035-5.

Cisek, A.A., Bak, I., Stefanska, I., Binek, M., 2022. Selection and optimization of high-yielding DNA isolation protocol for quantitative analyses of methanogenic archaea. Microorganisms 10 (3). https://doi.org/10.3390/microorganisms10030523.

Diender, M., Pereira, R., Wessels, H.J., Stams, A.J., Sousa, D.Z., 2016. Proteomic Analysis of the Hydrogen and Carbon Monoxide Metabolism of Methanothermobacter marburgensis. Front. Microbiol. 7, 1049. https://doi.org/10.3389/fmicb.2016.01049.

Dupnock, T.L., Deshusses, M.A., 2019. Detailed investigations of dissolved hydrogen and hydrogen mass transfer in a biotrickling filter for upgrading biogas. Bioresour. Technol. 290, 121780. https://doi.org/10.1016/j.biortech.2019.121780.

Dyksma, S., Gallert, C., 2019. Candidatus Syntrophosphaera thermopropionivorans: a novel player in syntrophic propionate oxidation during anaerobic digestion. Environ. Microbiol. Rep. 11 (4), 558–570. https://doi.org/10.1111/1758-2229.12759.

Dyksma, S., Jansen, L., Gallert, C., 2020. Syntrophic acetate oxidation replaces acetoclastic methanogenesis during thermophilic digestion of biowaste. Microbiome 8 (1), 105. https://doi.org/10.1186/s40168-020-00862-5.

Feickert Fenske, C., Kirzeder, F., Strubing, D., Koch, K., 2023a. Biogas upgrading in a pilot-scale trickle bed reactor - long-term biological methanation under real application conditions. Bioresour. Technol. 376, 128868. https://doi.org/10.1016/j.biortech.2023.128868.

Feickert Fenske, C., Strubing, D., Koch, K., 2023b. Biological methanation in trickle bed reactors - a critical review. Bioresour. Technol. 385, 129383. https://doi.org/10.1016/j.biortech.2023.129383.

Figueras, J., Benbelkacem, H., Dumas, C., Buffiere, P., 2021. Biomethanation of syngas by enriched mixed anaerobic consortium in pressurized agitated column. Bioresour. Technol. 338, 125548. https://doi.org/10.1016/j.biortech.2021.125548.

Gerardi, M.H. (2003). *The Microbiology of Anaerobic Digesters*. Wiley. https://books.google.se/books?id=QzzENAEACAAJ.

Goonesekera, E.M., Grimalt-Alemany, A., Thanasoula, E., Yousif, H.F., Krarup, S.L., Valerin, M.C., Angelidaki, I., 2024. Biofilm mass transfer and thermodynamic constraints shape biofilm in trickle bed reactor syngas biomethanation. Chem. Eng. J. 500. https://doi.org/10.1016/j.cej.2024.156629.

Grimalt-Alemany, A., Łężyk, M., Kennes-Veiga, D.M., Skiadas, I.V., Gavala, H.N., 2019. Enrichment of Mesophilic and Thermophilic mixed Microbial Consortia for Syngas Biomethanation: the Role of Kinetic and Thermodynamic Competition. Waste Biomass Valoriz. 11 (2), 465–481. https://doi.org/10.1007/s12649-019-00595-z.

Grimalt-Alemany, A., Skiadas, I.V., Gavala, H.N., 2017. Syngas biomethanation: state-of-the-art review and perspectives. Biofuels Bioprod. Biorefin. 12 (1), 139–158. https://doi.org/10.1002/bbb.1826.

Gu, W., Muller, A.L., Deutzmann, J.S., Williamson, J.R., Spormann, A.M., 2022. Growth rate-dependent coordination of catabolism and anabolism in the archaeon Methanococcus maripaludis under phosphate limitation. ISME J. 16 (10), 2313–2319. https://doi.org/10.1038/s41396-022-01278-9.

Hattori, S., Galushko, A.S., Kamagata, Y., Schink, B., 2005. Operation of the CO dehydrogenase/acetyl coenzyme a pathway in both acetate oxidation and acetate formation by the syntrophically acetate-oxidizing bacterium Thermacetogenium phaeum. J. Bacteriol. 187 (10), 3471–3476. https://doi.org/10.1128/JB.187.10.3471-3476.2005.

Jensen, M.B., Poulsen, S., Jensen, B., Feilberg, A., Kofoed, M.V.W., 2021. Selecting carrier material for efficient biomethanation of industrial biogas-CO2 in a trickle-bed reactor. J. CO2 Util. 51, 101611. https://doi.org/10.1016/j.jcou.2021.101611.

Kamravamanesh, D., Rinta Kanto, J.M., Ali-Loytty, H., Myllärinen, A., Saalasti, M., Rintala, J., Kokko, M., 2023. Ex-situ biological hydrogen methanation in trickle bed reactors: Integration into biogas production facilities. Chem. Eng. Sci. 269. https://doi.org/10.1016/j.ces.2023.118498.

Lackner, N., Wagner, A.O., Markt, R., Illmer, P., 2020. pH and Phosphate induced shifts in carbon flow and microbial community during thermophilic anaerobic digestion. Microorganisms 8 (2). https://doi.org/10.3390/microorganisms8020286.

Laguillaumie, L., Rafrafi, Y., Moya-Leclair, E., Delagnes, D., Dubos, S., Sperandio, M., Paul, E., Dumas, C., 2022. Stability of ex situ biological methanation of H2/CO2 with a mixed microbial culture in a pilot scale bubble column reactor. Bioresour. Technol. 354, 127180. https://doi.org/10.1016/j.biortech.2022.127180.

Larsson, A., Gunnarsson, I. & tengberg, F. (2019). *The GoBiGas Project - Demonstration of the production of Biomethane from Biomas via Gasification*. AB, G.E.

Li, C., Zhu, X., Angelidaki, I., 2021. Syngas biomethanation: effect of biomass-gas ratio, syngas composition and pH buffer. Bioresour. Technol. 342, 125997. https://doi.org/10.1016/j.biortech.2021.125997.

Liu, R., Hao, X., Wei, J., 2016. Function of homoacetogenesis on the heterotrophic methane production with exogenous H2/CO2 involved. Chem. Eng. J. 284, 1196–1203. https://doi.org/10.1016/j.cej.2015.09.081.

Lozupone, C., Knight, R., 2005. UniFrac: a new phylogenetic method for comparing microbial communities. Appl. Environ. Microbiol. 71 (12), 8228–8235. https://doi.org/10.1128/AEM.71.12.8228-8235.2005.

Luo, G., Wang, W., Angelidaki, I., 2013. Anaerobic digestion for simultaneous sewage sludge treatment and CO biomethanation: process performance and microbial ecology. Environ. Sci. Technol. 47 (18), 10685–10693. https://doi.org/10.1021/es401018d.

Mancipe-Jiménez, D.C., Costa, C., Márquez, M.C., 2017. Methanogenesis inhibition by phosphorus in anaerobic liquid waste treatment. Waste Treat. Recovery 2 (1), 1–8. https://doi.org/10.1515/lwr-2017-0001.

McMurdie, P.J., Holmes, S., 2013. phyloseq: an R Package for Reproducible Interactive Analysis and Graphics of Microbiome Census Data. PLoS One 8 (4), e61217. https://doi.org/10.1371/journal.pone.0061217.

Porte, H., Kougias, P.G., Alfaro, N., Treu, L., Campanaro, S., Angelidaki, I., 2019. Process performance and microbial community structure in thermophilic trickling biofilter reactors for biogas upgrading. Sci. Total Environ. 655, 529–538. https://doi.org/10.1016/j.scitotenv.2018.11.289.

Rachbauer, L., Voitl, G., Bochmann, G., Fuchs, W., 2016. Biological biogas upgrading capacity of a hydrogenotrophic community in a trickle-bed reactor. Appl. Energy 180, 483–490. https://doi.org/10.1016/j.apenergy.2016.07.109.

Ren, J., Liu, Y.-L., Zhao, X.-Y., Cao, J.-P., 2020. Methanation of syngas from biomass gasification: an overview. Int. J. Hydrogen Energy 45 (7), 4223–4243. https://doi.org/10.1016/j.ijhydene.2019.12.023.

Reysenbach, A.-L., Huber, R., Stetter, K.O., Davey, M.E., MacGregor, B.J. & Stahl, D.A. (2001). Phylum BII. Thermotogae phy. nov. In: Boone, D.R., Castenholz, R.W. & Garrity, G.M. (eds) *Bergey's Manual® of Systematic Bacteriology: Volume One : The Archaea and the Deeply Branching and Phototrophic Bacteria*. New York, NY: Springer New York. 369-387. https://doi.org/10.1007/978-0-387-21609-6_19.

Rother, M., Oelgeschlager, E., Metcalf, W.M., 2007. Genetic and proteomic analyses of CO utilization by Methanosarcina acetivorans. Arch. Microbiol. 188 (5), 463–472. https://doi.org/10.1007/s00203-007-0266-1.

Sancho Navarro, S., Cimpoia, R., Bruant, G., Guiot, S.R., 2016. Biomethanation of Syngas using Anaerobic Sludge: Shift in the Catabolic Routes with the CO Partial pressure increase. Front. Microbiol. 7, 1188. https://doi.org/10.3389/fmicb.2016.01188.

Sieborg, M.U., Jensen, M.B., Jensen, B., Kofoed, M.V.W., 2021. Effect of minimizing carrier irrigation on H2 conversion in trickle bed reactors during ex situ biomethanation. Bioresour. Technol. Rep. 16. https://doi.org/10.1016/j.biteb.2021.100876.

Singh, A., Schnurer, A., Dolfing, J., Westerholm, M., 2023. Syntrophic entanglements for propionate and acetate oxidation under thermophilic and high-ammonia conditions. ISME J. 17 (11), 1966–1978. https://doi.org/10.1038/s41396-023-01504-y.

Sipma, J., Lens, P.N.L., Stams, A.J.M., Lettinga, G., 2003. Carbon monoxide conversion by anaerobic bioreactor sludges. FEMS Microbiol. Ecol. 44 (2), 271–277. https://doi.org/10.1016/S0168-6496(03)00033-3.

Steinberg, L.M., Regan, J.M., 2008. Phylogenetic comparison of the methanogenic communities from an acidic, oligotrophic fen and an anaerobic digester treating municipal wastewater sludge. Appl. Environ. Microbiol. 74 (21), 6663–6671. https://doi.org/10.1128/AEM.00553-08.

Strübing, D., Huber, B., Lebuhn, M., Drewes, J.E., Koch, K., 2017. High performance biological methanation in a thermophilic anaerobic trickle bed reactor. Bioresoure Technology 245 (Pt A), 1176–1183. https://doi.org/10.1016/j.biortech.2017.08.088.

Thema, M., Weidlich, T., Kaul, A., Bollmann, A., Huber, H., Bellack, A., Karl, J., Sterner, M., 2021. Optimized biological CO2-methanation with a pure culture of thermophilic methanogenic archaea in a trickle-bed reactor. Bioresour. Technol. 333, 125135. https://doi.org/10.1016/j.biortech.2021.125135.

Wegener Kofoed, M.V., Jensen, M.B., Mørck Ottosen, L.D., 2021. Biological upgrading of biogas through CO2 conversion to CH4. In: In: *Emerging Technologies and Biological Systems for Biogas Upgrading*, pp. 321–362. https://doi.org/10.1016/b978-0-12-822808-1.00012-x.

Westerholm, M., Dolfing, J., Schnurer, A., 2019. Growth Characteristics and Thermodynamics of Syntrophic Acetate Oxidizers. Environ. Sci. Technol. 53 (9), 5512–5520. https://doi.org/10.1021/acs.est.9b00288.

Westerholm, M., Hansson, M., Schnurer, A., 2012. Improved biogas production from whole stillage by co-digestion with cattle manure. Bioresour. Technol. 114, 314–319. https://doi.org/10.1016/j.biortech.2012.03.005.

Westerholm, M., Isaksson, S., Karlsson Lindsjö, O., Schnürer, A., 2018. Microbial community adaptability to altered temperature conditions determines the potential for process optimisation in biogas production. Appl. Energy 226, 838–848. https://doi.org/10.1016/j.apenergy.2018.06.045.